Dynamic Fluctuations of Semiflexible Filaments

R. Everaers,[1,2] F. Jülicher,[1] A. Ajdari,[3] and A. C. Maggs[3]
[1]*Institut Curie, Physico-Chimie Curie, UMR CNRS/IC 168, 26 rue d'Ulm, 75248 Paris Cedex 05, France*
[2]*Max-Planck-Institut für Polymerforschung, Postfach 3148, D-55021 Mainz, Germany*
[3]*Physico-Chimie Théorique, Esa CNRS 7083, ESPCI, 10 rue Vauquelin, 75231 Paris Cedex 05, France*
(Received 4 August 1998)

We study both the longitudinal and transverse fluctuations of a semiflexible filament. Using scaling arguments and numerical simulations, we find several regimes for the longitudinal fluctuations which, for short times, scale as $\langle \delta r_\parallel^2 \rangle \sim t^{7/8}$ and are correlated over a length $l_2 \sim t^{1/8}$. Our results are pertinent to experiments on cross-linked filament systems and motor-filament assays. The techniques we develop for the analysis of dynamic correlations should have wide applications in the study of polymer systems. [S0031-9007(99)09052-3]

PACS numbers: 83.80.Lz, 83.10.Nn, 83.20.Jp

Advances in manipulation techniques of biopolymers allow the experimentalist to study and visualize the motion of semiflexible filaments such as DNA, actin and microtubules under the influence of thermal noise, solvent flows, and forces generated by motor proteins [1,2]. A first step towards the understanding of mechanical properties of elastic filaments are linear response functions which are related to dynamic fluctuations, via the fluctuation-dissipation theorem. For flexible polymers, the dynamics is well described by the Rouse and Zimm models and governed by the evolution of a single intrinsic length scale [3]. For semiflexible polymers a complete theory of the anisotropic motion is still lacking.

In this Letter, we present a full characterization of the dynamic fluctuations of semiflexible filaments. We show that the dynamics do not scale in the conventional manner and that two competing length scales govern the transverse and longitudinal fluctuations of stiff filaments. This surprising prediction is clearly demonstrated by numerical data which we have generated over 12 decades in time using a new simulation scheme and data-analysis techniques. Finally, we discuss situations where the newly predicted regimes for longitudinal motion are dominant.

A standard model of semiflexible polymers is the wormlike chain (WLC), $\mathcal{H} = \kappa/2 \int_0^L ds[\partial^2 \vec{r}(s)/\partial s^2]^2$, of an incompressible elastic rod with bending modulus κ and arclength s. For many biopolymers the contour lengths L of interest are of the order of the persistence length $L \simeq \kappa$ where thermal fluctuations begin to induce appreciable deviations from a straight rod. (Here and in the following, we use units for which $k_B T = 1$, as well as $\eta = 1$, where η is the friction coefficient of the filament per unit length. In these units time is a volume. For actin, $\kappa \simeq 20\ \mu$m and 1 s $\approx 1\ \mu$m^3.) WLCs behave qualitatively different from ordinary flexible polymers with $L \gg \kappa$, which are controlled by entropic tensions. In particular, the conformations and fluctuations of WLCs are highly anisotropic.

The static anisotropy in the WLC model is characterized by the exponent for the growth of transverse fluctuations, $\langle \delta r_\perp^2 \rangle \sim L^3/\kappa$, as a function of the filament length $L < \kappa$ [4]. Because of the conservation of filament length the transverse fluctuations result in longitudinal fluctuations $\langle \delta r_\parallel^2 \rangle \sim L^4/\kappa^2$. The fluctuation dissipation theorem relates the anisotropic fluctuations to a tensorial response function with eigenvalues $\lambda_\parallel = \langle \delta r_\parallel^2 \rangle$ and $\lambda_\perp = \langle \delta r_\perp^2 \rangle$, characterizing the effective bending and compressional elasticities, respectively. We shall generalize this statement to the dynamic response.

At linear order, the dynamics of a filament is commonly described by a Langevin equation for the transverse fluctuations alone:

$$\frac{\partial r_\perp}{\partial t} = -\kappa \frac{\partial^4 r_\perp}{\partial s^4} + f_\perp(s,t). \tag{1}$$

Here, $f_\perp$ denotes a transverse stochastic force and hydrodynamic interactions are neglected on the ground that they induce only logarithmic corrections. After time t, the filament is equilibrated over a length $l_1(t) \sim (\kappa t)^{1/4}$. This results in a scaling law for the transverse motion of a monomer [5] easily observed in dynamic light scattering [6] or microrheology [7]:

$$\langle \delta r_\perp(t)^2 \rangle \sim l_1(t)^3/\kappa \sim t^{3/4}/\kappa^{1/4}. \tag{2}$$

The longitudinal fluctuations of a filament are more subtle. Two different approaches exist in the literature: Approximating the incompressibility via a global Lagrange multiplier for the total length of the filament [8,9] leads to the prediction (2) for both the longitudinal and transverse motions, while taking the local constraint into account leads again to scaling in $t^{3/4}$, however, with an amplitude smaller by a factor L/κ than in Eq. (2) [10,11]. The latter result can be found with a simple scaling argument: Each section of length $l_1(t)$ of the filament is independent and contributes the static value $\langle \delta r_\parallel^2 \rangle(l_1) \sim l_1^4/\kappa^2$ to the mean square longitudinal fluctuations of the end of a filament:

$$\langle \delta r_\parallel(t)^2 \rangle \sim (L/l_1)(l_1^4/\kappa^2) = L t^{3/4}/\kappa^{5/4}. \tag{3}$$

The derivation of Eq. (3) neglects longitudinal friction. As demonstrated in [11], this is appropriate in a sheared sample where the longitudinal friction drops out of the dynamic equations leading to a scaling in $t^{3/4}$ in the high frequency shear modulus. For a filament in a quiescent solvent, however, longitudinal friction and local incompressibility cannot be neglected [12,13]. The shortening (or extension) of a filament section of length $l_1(t)$ also requires the longitudinal motion of its neighbors. As a consequence, longitudinal friction limits the number of sections which can contribute within a finite time: Consider the response of a filament to a weak constant longitudinal force $f_\parallel$ applied to the end. Equation (3) together with the fluctuation dissipation theorem predicts that the end drifts as $\delta r_\parallel(t) \sim f_\parallel L t^{3/4}/\kappa^{5/4}$. However, not the whole filament is set into motion at once: The velocity scales as $v_\parallel \sim \delta r_\parallel/t \sim f_\parallel L/\kappa^{5/4} t^{1/4}$, but clearly the total drag $L v_\parallel$ cannot be larger than the applied force. For a long filament we can resolve this paradox by assuming that the tension propagates a distance $l_2(t) \sim t^{1/8}\kappa^{5/8} < L$. Only a length l_2 is set into motion with a velocity of the order of $v_\parallel \sim f_\parallel/l_2$ and the end drifts a distance $\delta r_\parallel(t) \sim f_\parallel t^{7/8}/\kappa^{5/8}$. The fluctuation-dissipation theorem relates this response to the amplitude of longitudinal fluctuations:

$$\langle \delta r_\parallel^2(t) \rangle \sim t^{7/8}/\kappa^{5/8}. \tag{4}$$

Our surprising conclusion is that longitudinal and transverse dynamics are governed by two different dynamic length scales [14]. This suggests that the fluctuations of the filament ends obey a pair of scaling relations with different scaling arguments:

$$\langle \delta r_\parallel(t)^2 \rangle = \frac{t^{7/8}}{\kappa^{5/8}} \mathcal{Q}\left(\frac{t^{1/8}\kappa^{5/8}}{L}\right), \tag{5}$$

$$\langle \delta r_\perp(t)^2 \rangle = \frac{t^{3/4}}{\kappa^{1/4}} \mathcal{W}\left(\frac{t^{1/4}\kappa^{1/4}}{L}\right). \tag{6}$$

The scaling functions $\mathcal{Q}$ and $\mathcal{W}$ are constant for small arguments. For large arguments x, $\mathcal{Q}(x) \sim x$, $\mathcal{W}(x) \sim x$ if the filament can diffuse freely.

In order to test these predictions, we have performed simulations of a semiflexible polymer in two dimensions imposing a constraint on the contour length using the technique described in [15]. The polymer is discretized as a sequence of beads with positions $\vec{r}_i$, $i \in 0, \ldots, n$, with fixed distance $b = |\vec{r}_i - \vec{r}_{i-1}|$ and normalized bond vectors $\vec{d}_i = (\vec{r}_i - \vec{r}_{i-1})/b$. The angles θ_i characterizing the bond directions are coupled by simple angular springs: $E = \frac{1}{2}\sum_{i=1}^{n-1} \frac{\kappa}{b}(\theta_i - \theta_{i+1})^2$. The beads move against an isotropic friction $-b\partial\vec{r}_i/\partial t$ under the influence of the forces due to the angular springs, $-\partial E/\partial \vec{r}_i$ and stochastic forces $\vec{F}_i^{\mathrm{ra}}$:

$$b\frac{\partial \vec{r}_i}{\partial t} = -\frac{\partial E}{\partial \vec{r}_i} + \vec{F}_i^{\mathrm{ra}} + T_{i+1}\vec{d}_{i+1} - T_i\vec{d}_i\,. \tag{7}$$

The tensions T_i play the role of Lagrange multipliers whose values are calculated at each time step from the condition that the bond lengths are equal to b.

The shortest characteristic time of the model is approximately $\tau(b) = b^4/\kappa$, while the relaxation time of a chain of $n = L/b$ segments varies as $\tau_n \sim n^4\tau(b)$. The total simulation time needed to equilibrate a chain is proportional to n^5. The equilibration of long chains becomes quickly impossible.

We get around the problem of generating independent configurations by simulating long chains for a time *far* shorter than the equilibration time but then performing ensemble averages over many short runs (see Fig. 1). These simulations are useful because we can easily prepare *fully equilibrated* initial conformations by drawing bond angles $\delta\theta = \theta_i - \theta_{i-1}$ randomly from a Gaussian distribution $P(\delta\theta) \sim \exp(-\frac{\kappa}{2b}\delta\theta^2)$. The choice of the segmentation then determines a window of accessible time scales. The elementary time step of the integrator is $10^{-2}\tau(b)$; times shorter than $\tau(b)$ are affected by discretization errors. We generated data for times up to $10^3\tau(b)$ with a computational effort proportional to only n^1. We chose a sequence of segmentations $b_j = 2^{-j}\kappa$ and studied chains of length $\kappa/8, \kappa/4, \kappa/2, \kappa$ with the number of segments varying between $n = 8$ and $n = 512$. The overlap between adjacent time windows ($\tau_n = 2^4\tau_{n/2}$) provides a convenient check on the coarse graining procedure and the scaling of the parameters.

Imposing a constraint on the bond lengths provides access to longer times than simulations done with stiff longitudinal springs without changing the results beyond the relaxation time of the high frequency Rouse modes (see Fig. 2) [16]. Indeed, we avoid simulating these fast but uninteresting modes which limit the integration step in any explicit integration scheme. There are nevertheless severe complications [15]; we must add a pseudopotential [17], $-\frac{1}{2}\log(\Delta)$ to E and include the corresponding forces in (7): Δ is the determinant of the Jacobian describing the transformation from Cartesian to bond angle coordinates. A proper calculation of these forces is essential to ensure

FIG. 1. Cloud of end points generated by simulating $N = 100$ realizations of the dynamics starting from the illustrated initial condition. The moments of this cloud are used to distinguish the longitudinal and transverse dynamics. The transverse fluctuations are larger in amplitude than the longitudinal fluctuations.

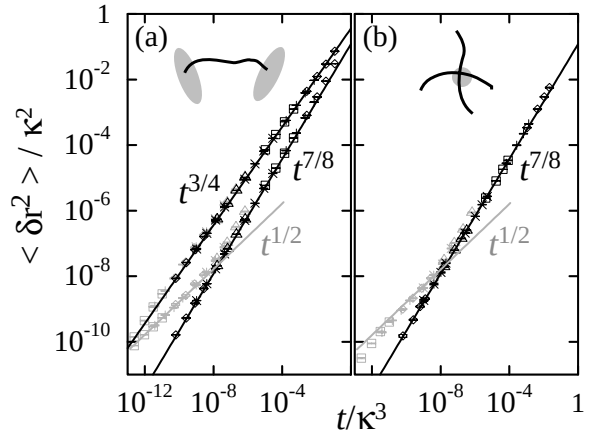

FIG. 2. (a) Amplitude of a filament end fluctuations as a function of time for an incompressible filament (black symbols, $L = \kappa$) determined from the moments $\lambda_1(t)$, $\lambda_2(t)$ of the 2D clouds. The transverse fluctuations scale as $\langle \delta r_\perp^2 \rangle = \lambda_1(t) \sim t^{3/4}$, while the longitudinal modes obey initially $\langle \delta r_\parallel^2 \rangle = \lambda_2(t) \sim t^{7/8}$. The scaling of the crossover to free diffusion at $L = l_2(t)$ is treated in Fig. 3. For compressible filaments (grey symbols, $L = \kappa/4$, modulus $K = 10^7 \kappa^{-1}$) a Rouse-like scaling $\lambda_2(t) = \langle \delta r_\parallel^2 \rangle \sim t^{1/2}$ is found for short times. (b) Isotropic fluctuations of a cross-linked filament pair scale as $\langle \delta r_\times^2 \rangle \sim t^{7/8}$. Different symbols correspond to different levels of coarse graining.

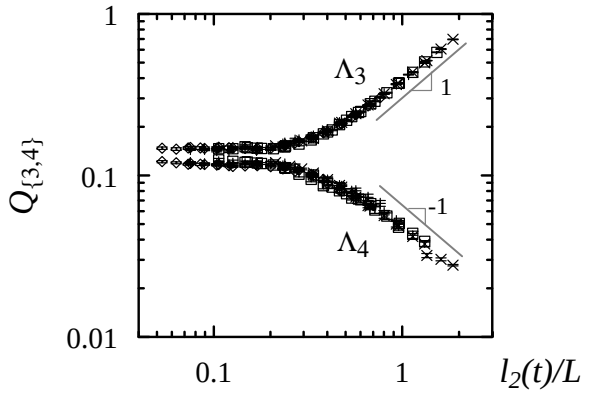

FIG. 3. Scaling behavior of the two smallest moments $\Lambda_{3,4}$ of the 4D clouds. The scaled amplitude $\mathcal{Q}_{\{3,4\}} = \Lambda_{\{3,4\}} \kappa^{5/8} t^{-7/8}$ is shown as a function of the tension propagation length $l_2(t) = t^{1/8} \kappa^{5/8}$ for $L = \kappa$ ($\diamond$), $\kappa/2$ (+), $\kappa/4$ ($\square$), $\kappa/8$ ($\times$). The plot confirms the scaling form of Eq. (5).

that we start our short runs from initial conformations which are properly equilibrated.

The objective of our simulations is the characterization of the transverse and longitudinal motion and the full tensorial response of the chain ends. For this purpose we perform N simulations (typically $N = 1000$) starting from an identical preequilibrated conformation; each simulation uses an independent series of random forces. We then record the N coordinates of one end of the chain as a function of time which form an evolving two-dimensional cloud in the (x, y) plane. The moments, $\lambda_1 > \lambda_2$, and axis of inertia of the point cloud characterize the amplitude and direction of transverse and longitudinal movement, respectively, for the given initial conformation (see Fig. 1).

We prepare a total of M random realizations (typically $M = 100$) of the initial chain over which we can calculate average properties of the cloud performing a total of $MN = 10^5$ simulations [see Fig. 2(a)]. For short times, the evolution of the cloud is very anisotropic, and the transverse dynamics corresponds to the larger moment $\lambda_1(t) = \langle \delta r_\perp^2 \rangle$ which scales according to Eq. (2). The smaller moment $\lambda_2(t) = \langle \delta r_\parallel^2 \rangle$ characterizes the longitudinal motions of the filament and for short times varies in agreement with our prediction [Eq. (4)]. For long times with $l_2 > L$, a length-dependent crossover to free diffusion of the whole filament occurs (see Fig. 3 for the crossover scaling). In addition, the analysis shows that the direction of the longitudinal motion is initially parallel to the *local* tangent and relaxes only with time towards the average orientation of the whole filament. This tilt angle between the initial tangent and the average orientation of the chain is of the order of $\langle \psi^2 \rangle \sim L/\kappa$. Relaxation to the average orientation occurs only when $l_1(t) \sim L$. Fluctuations projected onto the average orientation of the whole filament, $\langle \delta r_\parallel^2 \rangle + \langle \psi^2 \rangle \langle \delta r_\perp^2 \rangle$, are dominated by the contribution of *transverse* motion for short times. They are an incorrect measure of the underlying longitudinal dynamics. However, fluctuations projected on the initial local tangent vector are dominated by the longitudinal dynamics and scale as $t^{7/8}$.

To better understand the tension propagation, we examined the joint motion of the two end points of a chain. In a series of M simulations, one generates a distribution of points in four dimensions (4D): $\{[x(0), x(L), y(0), y(L)]\}$. We are interested in the evolution of the four moments $\{\Lambda_1 > \Lambda_2 > \Lambda_3 > \Lambda_4\}$ of the 4D cloud which characterize the dynamics of the whole chain.

Our picture of the propagation of tension fluctuations as introduced above suggests the following scenario: As long as $l_2 < L$, the movement of the ends are uncorrelated. The 4D distribution factorizes and reduces to a product of the 2D case discussed above: The two smaller moments $\Lambda_3 \simeq \Lambda_4 \simeq \langle \delta r_\parallel^2 \rangle$ and scale as $t^{7/8}/\kappa^{5/8}$; the two larger moments $\Lambda_1 \simeq \Lambda_2 \simeq \langle \delta r_\perp^2 \rangle$ scale as $t^{3/4}/\kappa^{1/4}$. For longer times $l_2(t) > L$ the two ends see each other as tension propagates along the filament. This lifts the degeneracy between Λ_3 and Λ_4, with Λ_4 now characterizing the end to end fluctuations so that according to (3) $\Lambda_4 \sim L t^{3/4}/\kappa^{5/4}$, and $\Lambda_3 \sim t/L$ characterizing the longitudinal free diffusion of the chain. Figure 3 shows the moments Λ_3 and Λ_4 plotted normalized by $t^{7/8}/\kappa^{5/8}$ as functions of $t^{1/8}\kappa^{5/8}/L$, so that they clearly follow the scaling form Eq. (5) [18].

How can one observe the motion corresponding to $\Lambda_{3,4}$ which scales as $t^{7/8}$? Naively, one might expect it to

be subdominant compared to $\Lambda_{1,2}$ in most experimental situations. However, a case where it dominates is a pair of cross-linked filaments confined to a quasi-two-dimensional region (a standard experimental setup for fluorescence microscope studies of actin filaments). The mean-square displacements of the cross-link are determined by the sum of the *inverse* response functions of the two chains (the sum of the effective elastic moduli) and is thus dominated by the stiff longitudinal response. Cross-link motion should therefore scale as $\langle \delta r_{\times}^2 \rangle \sim t^{7/8}$. We have checked this argument by simulating filament pairs of length L in two dimensions cross-linked perpendicularly at their midpoints [see Fig. 2(b)]. The motion of the cross-link is isotropic, and its amplitude $\langle \delta r_{\times}^2 \rangle$ is indeed numerically almost identical to $\langle \delta r_{\parallel}^2 \rangle$ for a single filament. This example of the cross-link demonstrates that the full response function is needed to estimate effective elasticities in cross-linked geometries, the knowledge of a single component of the tensor being insufficient.

Anisotropic response functions are also expected to be important for understanding filament pulling experiments using micromanipulation techniques or for studies of the action of myosin molecular motors. Myosin molecules can generate forces and displacements parallel to the local tangent of actin filaments. The resulting filament motion is then determined by the longitudinal response function discussed above. In some micromanipulation experiments on myosin function, actin filaments are used as force transducers [2]: The motion of one of the ends is an indicator for forces induced somewhere along the filament. The first response should be due to tension propagation and our prediction for $l_2(t)$ should thus characterize the transmission of information in a dynamic filament. Indeed tension propagation leads to an effective low-frequency filter since filament motion observed at a distance L is characterized by the longitudinal response function which is zero for times shorter than L^8/κ^5.

The anisotropic scaling of the dynamics predicted here could also be observable in incoherent neutron scattering experiments on stiff synthetic polymers. Recent work has shown that effects of semiflexibility are observable in these systems [9]. We expect that for long times the incoherent structure factor shows a behavior characterized by longitudinal modes.

Finally, we have presented a novel scheme of simulation and data analysis. Rather than following a single trajectory in configuration space for a very long time, we perform short, independent runs from equilibrated initial configurations and gain access to a wide range of time scales by varying the discretization of the model. To properly account for the anisotropy, we obtain the dynamic correlations by averaging over independent runs from *identical* initial configuration, *before* calculating ensemble averages. These techniques have the advantage of directly separating the nature of the different relaxation processes in our simulations and will also be useful for other machine studies of polymer dynamics.

We would like to thank Paul Chaikin, Fred Gittes, Fred Mackintosh, David Morse, and Jacques Prost for discussions on this work.

[1] F. Gittes, B. Mickey, J. Nettleton, and J. Howard, J. Cell Biol. **120**, 923 (1993); T. T. Perkins, D. E. Smith, and S. Chu, Science **264**, 819 (1994); J. Kas *et al.,* Biophys. J. **70**, 609 (1996).

[2] J. T. Finer, R. M. Simmons, and J. A. Spudich, Nature (London) **368**, 113 (1994).

[3] M. Doi and S. F. Edwards, *The Theory of Polymer Dynamics* (Clarendon Press, Oxford, 1986).

[4] T. Odjik, Macromolecules **16**, 1340 (1983).

[5] E. Farge and A. C. Maggs, Macromolecules **26**, 5041 (1993).

[6] C. F. Schmidt, M. Bärmann, G. Isenberg, and E. Sackmann, Macromolecules **22**, 3638 (1989).

[7] F. Amblard, A. C. Maggs , B. Yurke, A. Pargellis, and S. Leibler, Phys. Rev. Lett. **77**, 4470 (1996).

[8] J. Harris and J. Hearst, Chem. Phys. **44**, 2595 (1966).

[9] L. Harnau, R. G. Winkler, and P. Reineker, J. Chem. Phys. **106**, 2469 (1997).

[10] F. Gittes and F. Mackintosh, Phys. Rev. E **58**, R1241 (1998); R. Granek, J. Phys. II (France) **7**, 1761 (1997).

[11] D. Morse, Phys. Rev. E **58**, R1237 (1998); Macromolecules **31**, 7030 (1998); Macromolecules **31**, 7044 (1998).

[12] U. Seifert, W. Wintz, and P. Nelson, Phys. Rev. Lett. **77**, 5389 (1996).

[13] A. Ajdari, F. Jülicher, and A. C. Maggs, J. Phys. I (France) **47**, 1823 (1997).

[14] The scaling with two length scales is related to the expansion about an ordered (straight) state in a system with no real long range order. An analogous situation exists in the dynamics of the one- and two-dimensional Heisenberg model [see G. Reiter, Phys. Rev. B **21**, 5356 (1980)].

[15] E. J. Hinch, J. Fluid Mech. **271**, 219 (1994); P. S. Grassia, E. J. Hinch, and L. C. Nitsche, J. Fluid Mech. **282**, 373 (1995); P. S. Grassia and E. J. Hinch, J. Fluid Mech. **308**, 255 (1996).

[16] In three dimensions there is also a torsional mode which produces even richer behavior and will be treated in a future publication.

[17] M. Fixman, J. Chem. Phys. **69**, 1527 (1978).

[18] The short time splitting between Λ_3 and Λ_4 in Fig. 3 is partly due to fluctuations of order of $1/N^{1/2}$ and partly intrinsic due to the nonharmonicity of the corresponding elasticity.